

Natural time analysis of critical phenomena: The case of acoustic emissions in triaxially deformed Etna basalt

F. VALLIANATOS^[1,2], G. MICHAS^[1,2], P. BENSON^[3], and P. SAMMONDS^[1]

1 University College London, Gower Str., London, WC1E 6BT, UK

2 Technological Educational Institute of Crete, Laboratory of Geophysics and Seismology, Crete, Greece

3 University of Portsmouth, UK

PACS numbers.

89.75.Da Systems obeying scaling laws

89.75.-k Complex systems

91.30.Px Earthquakes

Abstract

Acoustic emissions exhibit complex correlations between space, time, and magnitude and as such they present a unique example for a complex time series. We apply the recently introduced method of natural time analysis, which enables the detection of long-range temporal correlations even in the presence of heavy tails and find that the acoustic emissions exhibits features similar to that of other equilibrium or non-equilibrium critical systems such as the worldwide seismicity as presented in the Centennial earthquake catalogue which includes global seismicity event with magnitude $M_w > 7.0$.

It is recognized that earthquake is the failure of the focal earth material accompanied by a rapid release of moment. Similarly, the acoustic emissions (AEs) in a rock experiment, are elastic waves generated in conjunction with energy release during crack onset, propagation and internal deformations in rock's body. Experiments of rock deformation are considered as a tool for understanding the occurrence of natural earthquakes [1]. Acoustic emission studies can give us an insight into the fracture network evolution processes that take place and provide us with the opportunity to develop laws suitable for testing at larger scales [1]. The latter could be useful in understanding earthquake mechanisms and may contribute to solving the problem of earthquake prediction [2].

Fracturing is one of the most important examples of a complex process in heterogeneous materials involving a wide range of time and length scales, from the micro- to the structural scale. This process is governed by the nucleation, growth and coalescence of microcracks, eventually leading to failure. In this context, fracture can be seen as the outcome of the irreversible dynamics of a long-range interacting, disordered system. [3]

During rock deformation, energy released as high-frequency AE from microfractures within the sample. These emissions provide a passive indicator of the progression of inelastic damage, during the approach to failure. Characterisation of the sources that produce AE can provide us with an insight into the microscopic processes that are involved in the initiation and coalescence of damage within a loaded rock sample. Laboratory AE exhibit some remarkable similarities with large scale seismological events and earthquake physics, such as power law, frequency-magnitude distributions and Omori law aftershock behaviour [4-6]. Monitoring and characterisation of AE during experiments can improve our understanding of a wide range of processes, including fault asperity rupture and volcano-seismic events [7-9]. Recently this spatio-temporal similarity has been viewed in the frame of non-extensive statistical physics [10] in addition to the views where brittle fracture has been associated with a first-order transition [11-13] or to a critical point phenomenon [14]. We note that both the aforementioned approaches lead to power-law distributions since second-order transitions present scaling close to the critical point, while the first-order transitions follow scaling laws when the range of interactions is large [15]

The main motivation of our work is to investigate fracture in a heterogeneous brittle material (Etna basalt) under triaxial deformation, analyzing the temporal correlation of moment release of AE from microfractures that occur before the final fracture. We focus on the analysis of acoustic emissions in natural time [16-20]. We apply natural time analysis because it has been shown [18] that the analysis of time series of complex systems in this time domain reduces uncertainty and extracts signal information as much as possible. Natural time analysis enables [18-19] among others, the identification of long-range correlations even in the presence of "heavy tails" [21]. In addition, since the applications of this new type of analysis with interesting results have been presented in a variety of cases including seismicity [see 18 and the references therein, 21-28] and self-organized criticality, [29-32] the question whether fracture (i.e., AEs) is described by natural time parameters, even at the phenomenological level presents a challenge, possibly leading to a universal principle from rocks crack up to geodynamic scale.

High-speed multi-channel waveform recording technology enables us to monitor the spatio-temporal evolution of fracturing processes using AEs activity in triaxially deformed rock samples with high precision. [7-9]. Here we study acoustic emissions catalogue collected in laboratory experiments on highly fractured samples of Etna basalt, a porphyritic, alkali, lava-flow basalt from Mount Etna, Italy, which comprises millimetre-sized phenocrysts of pyroxene, olivine and feldspar in a fine-grained groundmass [7-9] deformed at a constant axial strain rate of $5 \times 10^{-6} \text{ s}^{-1}$ and at an effective confining pressure of 40 MPa. Previous studies [8] have shown that the Etna basalt used in this study contains a ubiquitous network of pre-existing microcracks, which are distributed relatively isotropically with the opening of new, dilatant microcracks to be present with their long axes parallel to the σ_1 direction.

Figure 1a shows the AEs magnitude M_{AE} similar defined in earthquakes, versus time. We observe that AE are mainly observed in the final stage of deformation in consistency with that stated in [7-9] that rapid

acceleration to failure often observed in the final phase of triaxial deformation of brittle rocks is accompanied by a fast increase in AE activity. The record between the arrows A and B (figure 1a), which spans the period of crack growth and dynamic failure, has used to analyse AE in natural time. As reported in [7-9] within the period A-B microcracks appear to nucleate in the lower right-hand part of the sample and then propagate to the upper left-hand part of the sample with the bulk of the total acoustic emission activity from the whole experiment to contained within this period. As presented in figure 1c, during the period A-B the cluster of AE propagates diagonally across the whole sample.

The natural time analysis of a complex system presented for first in [16] and in detailed in [18]. Here we recapitulate the concept of natural time analysis as applied in acoustic emission data. In a time series consisting of N acoustic emissions, the *natural time* χ serves as an index for the occurrence of the k^{th} event and is defined as $\chi_k = k/N$. For the analysis of AE the pair (χ_k, M_k) is considered, where M_k is the seismic moment released during the k^{th} event. Considering the evolution of (χ_k, M_k) , the continuous function $F(\omega)$ is defined as: $F(\omega) = \sum_{k=1}^N M_k \exp\left(i\omega \frac{k}{N}\right)$ (1), where $\omega = 2\pi\phi$ and ϕ stands for the *natural frequency*.

We normalize $F(\omega)$ dividing it by $F(0)$, $\Phi(\omega) = \frac{\sum_{k=1}^N M_k \exp\left(i\omega \frac{k}{N}\right)}{\sum_{n=1}^N M_n} = \sum_{k=1}^N p_k \exp\left(i\omega \frac{k}{N}\right)$ (2), where $p_k = M_k / \sum_{n=1}^N M_n$.

The quantities p_k describe a probability to observe the acoustic event at *natural time* χ_k . From (2) a normalized power spectrum can be obtained: $\Pi(\omega) = |\Phi(\omega)|^2$. For natural frequencies ϕ less than 0.5, $\Pi(\omega)$ or $\Phi(\omega)$ reduces to a characteristic function for the probability distribution p_k in the context of probability theory. It has been shown [18] that the following relation holds:

$$\Pi(\omega) = \frac{18}{5\omega^2} - \frac{6 \cos \omega}{5\omega^2} - \frac{12 \sin \omega}{5\omega^3} \quad (3)$$

According to the probability theory, the moments of a distribution and hence the distribution itself can be approximately determined once the behavior of the characteristic function of the distribution is known around zero.

For $\omega \rightarrow 0$, (3) leads to: $\Pi(\omega) \approx 1 - \kappa_1 \omega^2$ (4), where κ_1 is the variance in natural time given as $\kappa_1 = \langle \chi^2 \rangle - \langle \chi \rangle^2 = \sum_{k=1}^N p_k \chi_k^2 - \left(\sum_{k=1}^N p_k \chi_k\right)^2$ (5).

The quantity κ_1 has been proposed [18] as an order parameter for seismicity, based on three important findings: (a) The quantity κ_1 abruptly changes acquiring values very close to zero, once a final fracture (i.e a strong earthquake in case of seismicity) takes place, (b) when studying the fluctuations of κ_1 through an events catalogue using its *scaled probability distribution function* a universal curve appears and (c) the resulting universal curve exhibits fluctuations similar with those observed for other equilibrium and non-equilibrium critical systems.

When studying an acoustic emissions catalogue comprising W events by using a sliding natural time window of length l and examine the window starting at $k = k_0$, the quantities $p_j = M_{k_0-j-1} / \sum_{m=1}^l M_{k_0+m-1}$ are well defined and give rise to an average value μ_j equal to:

$$\mu_j = \frac{1}{W-l+1} \sum_{k_0=1}^{W-l+1} \frac{M_{k_0+j-1}}{\sum_{m=1}^l M_{k_0+m-1}} \quad (6)$$

The second order moments of p_j , as the variance is given as : $Var(p_j) = \frac{1}{W-l+1} \sum_{k_0=1}^{W-l+1} \left(\frac{M_{k_0+j-1}}{\sum_{m=1}^l M_{k_0+m-1}} - \mu_j \right)^2$, while the covariance [18, 21] is calculated by the expression :

$$Cov(p_j, p_i) = \frac{1}{W-l+1} \sum_{k_0=1}^{W-l+1} \left(\frac{M_{k_0+j-1}}{\sum_{m=1}^l M_{k_0+m-1}} - \mu_j \right) \times \left(\frac{M_{k_0+i-1}}{\sum_{m=1}^l M_{k_0+m-1}} - \mu_i \right)$$

Then the expectation value of κ_1 [18, 21] is expressed as :

$$E(\kappa_1) = \frac{1}{W-l+1} \sum_{k_0=1}^{W-l+1} \left\{ \sum_{j=1}^l \left(\frac{j}{l} \right)^2 \frac{M_{k_0+j-1}}{\sum_{m=1}^l M_{k_0+m-1}} - \left[\sum_{j=1}^l \left(\frac{j}{l} \right) \frac{M_{k_0+j-1}}{\sum_{m=1}^l M_{k_0+m-1}} \right]^2 \right\} \quad (7)$$

obtained from the $W-l+1$ windows of the acoustic emissions catalogue and is given by:

$$E(\kappa_1) = \kappa_{1,M} + \sum_{j=1}^{l-1} \sum_{i=j+1}^l \frac{(j-i)^2}{l^2} Cov(p_j, p_i) \quad (8),$$

where $\kappa_{1,M}$ is the value obtained from equation (5) when substituting μ_k for p_k , [21].

Natural time analysis enables the identification and quantification of magnitude correlation in a catalogue of acoustic emissions in matter analogue of that of seismicity [21], by comparing the value of $E(\kappa_1)$ of the original AE series with the distribution obtained for $E(\kappa_{1,shuf})$ when many randomly shuffled copies of the original AE catalogue used. Following the latter approach we consider a randomly shuffled copy of the original AEs catalogue, expecting that all p_j to be equivalent independent of j and thus $\mu_j = 1/l$. It has been shown [18] that the expectation value for κ_1 , denoted by $E(\kappa_{1,shuf})$ in the ensemble of randomly shuffled copy case, is given by:

$$E(\kappa_{1,shuf}) = \kappa_u \left(1 - \frac{1}{l^2} \right) - \kappa_u (l+1) Var(p) \quad (8), \text{ where } \kappa_u = 1/12 \text{ corresponding to a uniform distribution and } Var(p) \text{ the expectation value for } (p_j - 1/l)^2 \text{ in the shuffled catalogues.}$$

Comparing equations (8) and (9) we result that the difference between the value of $E(\kappa_1)$ of the original AE catalogue and the corresponding values obtained from randomly shuffled copies of the same catalogue results from the presence of magnitude correlations between successive AE within the window length l .

To identify the presence of magnitude correlations in AEs catalogue we apply the method proposed in [18,21] which is based on the following steps: first we consider a large number of *shuffled* copies of the original AE catalogue in order to determine the values $E(\kappa_1)$ through equation (7) in each case for the window length l . The latter enables the construction of a probability density function $f(\kappa_1)$, which is usually Gaussian characterized by a mean value μ and a standard deviation σ . If the value $E(\kappa_1)$ obtained from the *original* AEs catalogue is unlikely to result from $f(\kappa_1)$ or equivalently from the corresponding cumulative distribution function (CDF) $F(\kappa_1)$, then we identify the presence of magnitude correlations in the AE catalogue. If $f(\kappa_1)$ is Gaussian, the z-score $z = (E(\kappa_1) - \mu) / \sigma$ provides a measure of the disparity between actual and randomly shuffled data. To apply the procedure a window lengths $l = 6$ to 40 is used [18] and the average found from the totality of the κ_1 values is compared with the corresponding value obtained upon randomly shuffling the AE catalogue.

The representation of the AE Catalogue in natural time is given in Figure 1c. It comprises $W=1083$ acoustic emissions. We first search on the existence of an exponential tail which is a characteristic property of various critical systems. We consider in accordance to [18 and references therein], the natural time windows of lengths $l=6$ to 40 consecutive AE events. We start from the first AE event, calculate the $35\kappa_1$ values resulting from the first $l=6$ to 40 consecutive events. We next turn to the second AE and repeat the calculation of κ_1 . After sliding, event by event, through the whole AE catalogue, this procedure can be followed for 1044 ($=W-39$) times, amounting to 36540 [$=35\times(W-39)$] calculated κ_1 values, used to construct the probability density function $p(\kappa_1)$ presented in figure 2a with black circles, as well as the estimation of the average value $E(\kappa_1)$ and the standard deviation $\sigma(\kappa_1)$. As suggested in [18] the statistical properties of κ_1 (i.e. of the order parameter in natural time) could be studied by means of the scaled probability distribution function $P(y) \equiv \sigma(\kappa_1)p(\kappa_1)$. Figure 2b depicts with circles the scaled probability distribution function $P(y)$ versus the reduced κ_1 defined by $y = [E(\kappa_1)-\kappa_1]/\sigma(\kappa_1)$ for the AE catalogue for the period AB as presented in natural time (figures 1b). In figures 3a and 3b we reproduce for comparison the corresponding results of the distributions $p(\kappa_1)$ and $P(y)$ obtained from the Centennial Earthquake Catalogue for the period 1900 to September 30, 2007 as reported in [21] for a global seismicity with $M_w > 7.0$, along with that of AEs from Etna Basalts. An inspection of figure 3 reveals a remarkable coincidence, suggesting a possible universality between the curves corresponding to the AE catalogue and the Centennial Earthquake one. Moreover, the scaled probability density function of the AE Catalogue shares the characteristic exponential tail of various equilibrium and non-equilibrium critical systems in agreement with the results presented in [21] for the Centennial Earthquake Catalogue. .

We now proceed to the identification of the presence of magnitude correlations in the AE Catalogue. Following the method suggested in [18] and recapitulated here, we randomly shuffled the AE Catalogue for $n_1 = 10^3$ times and estimated for each randomly shuffled copy the average value of κ_1 , labeled $E(\kappa_{1,shuf})$, resulting from all the possible windows of lengths $l=6$ to 40. In figures 2a and 2b the results obtained for each shuffled AE catalogue are indicated by a gray line along with the values obtained from the analysis of the original AE data. By using the Kolmogorov-Smirnov-Lilliefors test, we found that the resulting $E(\kappa_{1,shuf})$ values follow the Gaussian distribution with mean $\mu_s = 0.0573$ and standard deviation $\sigma = 0.00097$. On the other hand, the original AE Catalogue results in an average κ_1 value $\mu_0=0.0614$, thus the estimated value of the z-score is $z = 4.215$ which differs markedly from zero, indicating the presence of temporal correlation. The latter implies that it is highly unlikely that μ_0 comes from the distribution of $E(\kappa_{1,shuf})$. The reason for this deviation is that as suggested in [18], μ_0 provides a measure of the presence of long-range correlations in the original AEs. Once these correlations are destroyed by randomly shuffling the data, the resulting $E(\kappa_{1,shuf})$ values differ significantly from μ_0 .

As an additional check for the validity of the above result we depict in Figure 4, the cumulative distribution function $F(\kappa_1)$ of $E(\kappa_{1,shuf})$ obtained from $n_2 = 10^3$ randomly shuffled copies of the AE Catalogue together with

the original μ_0 value indicated by a vertical line. A detailed inspection of Fig. 4 reveals that since μ_0 lies far above of the values of $E(\kappa_{1,shuf})$ it is unlikely to come from the distribution of them.

Summarizing we can state that the natural time analysis of the AE catalogue revealed that the order parameter κ_1 of the AE shares a characteristic feature similar to that of other equilibrium or non-equilibrium critical systems—including self-organized critical systems. The presence of the exponential tail in a scaled probability distribution function for AEs catalogue (i.e of the fracture evolution) has been shown when considering $\Pi(\varphi)$ for $\varphi \rightarrow 0$ or equivalently κ_1 as an order parameter for fracturing as indicating by the analysis of AEs. Our results indicate that AEs exhibits a similar behavior with that observed with earth seismicity [18-26]. We note that the latter similarity has to be viewed within the frame of a recent result [10] which suggests the nonextensive character of AEs with analogy with that observed in seismicity [33]. Here we conclude using the natural time approach (which focuses on the sequential order of the events that appear in nature) the existence of magnitude correlation of AEs in fully agreement with global seismicity's results [21]. Note also such a picture of non-trivially since it is support the universal behaviour of earth complex systems from crack evolution in laboratory scale to that of Earth's lithospheric activity.

Acknowledgments: This work was supported in part by the THALES Program of the Ministry of Education of Greece and the European Union in the framework of the project entitled "Integrated understanding of Seismicity, using innovative Methodologies of Fracture mechanics along with Earthquake and non-extensive statistical physics - Application to the geodynamic system of the Hellenic Arc. SEISMO FEAR HELLARC".

Figure 1

- a) The AE record of the Etna basalt deformed at 40 MPa effective pressure. The strain softening between peak stress and dynamic failure noted with the A and B arrows A – B
- b) AE event locations over the period AB . Colours indicate the moment magnitude of the AE
- c) The AE event over the period AB as presented in natural time

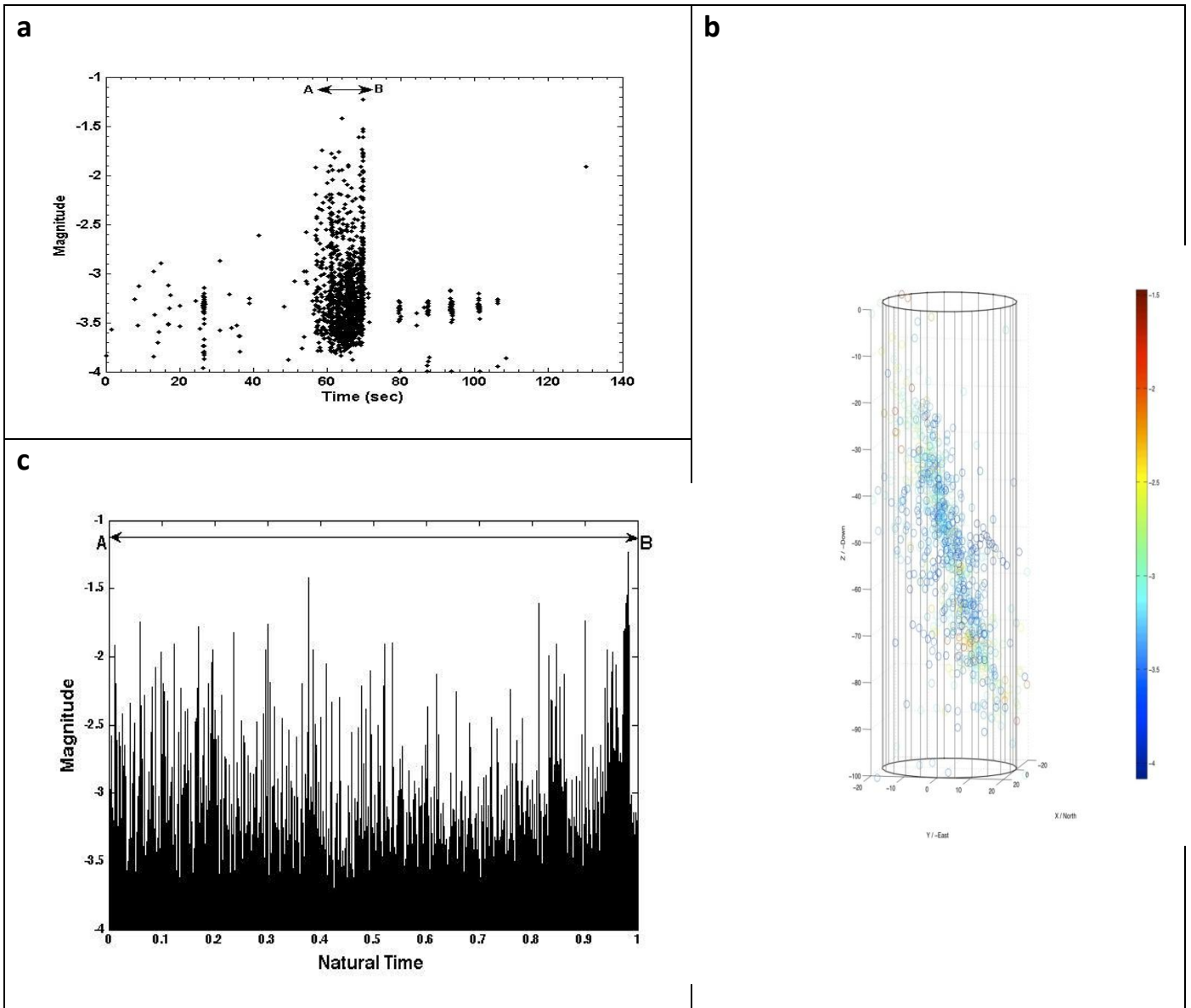
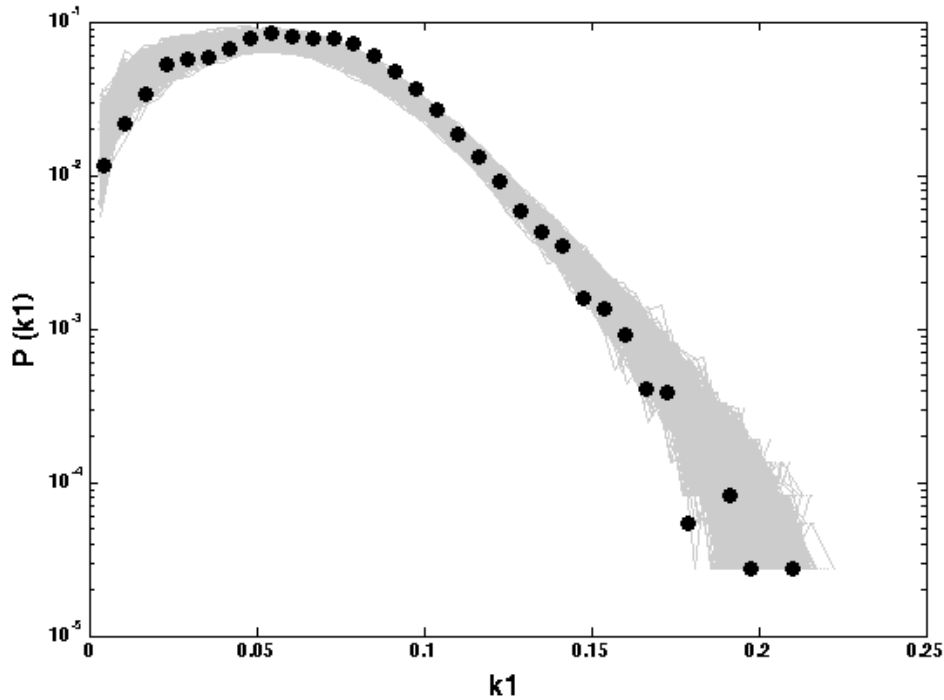


Figure 2

- a) The probability density function $\rho(\kappa_1)$ vs κ_1 (black circles) extracted from the analysis of the AE recorded in the AB period of the original AE catalogue. The gray lines present $\rho(\kappa_1)$ as estimated from the analysis of each shuffled AE catalogue created from the original AE data.



- b) The scaled probability distribution function $\mathcal{P}(y) \equiv \sigma(\kappa_1)\rho(\kappa_1)$ versus the reduced κ_1 defined by $y = [E(\kappa_1) - \kappa_1] / \sigma(\kappa_1)$ (black circles) extracted from the analysis of the AE recorded in the AB period of the original AE catalogue. The gray lines present $\mathcal{P}(y)$ as estimated from the analysis of each shuffled AE catalogue created from the original AE data.

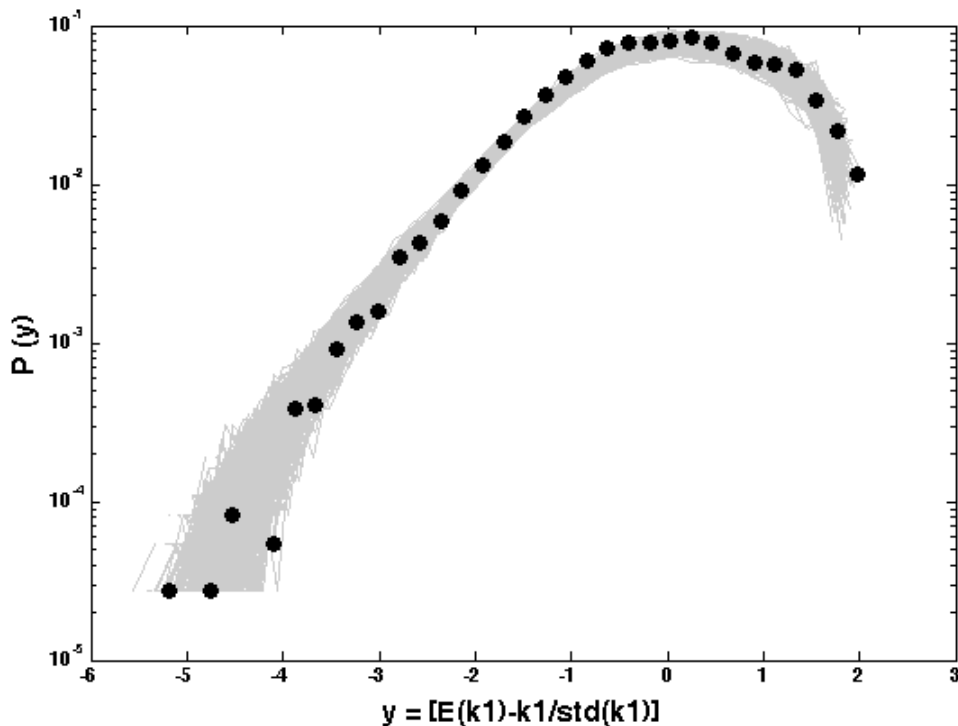


Figure 3

Comparison of the probability density function $p(\kappa_1)$ (figure 3a) and of the scaled probability distribution function $P(y)$ for the AE catalogue from Etna Basalts and for the period AB with that obtained from the Centennial Earthquake Catalogue for the period 1900 to September 30, 2007 for a global seismicity with $M_w > 7.0$.

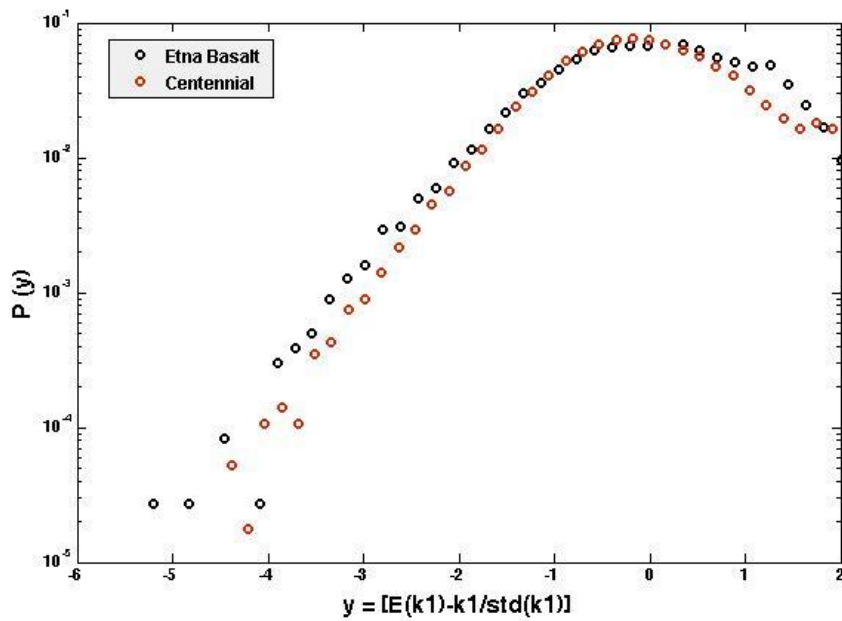
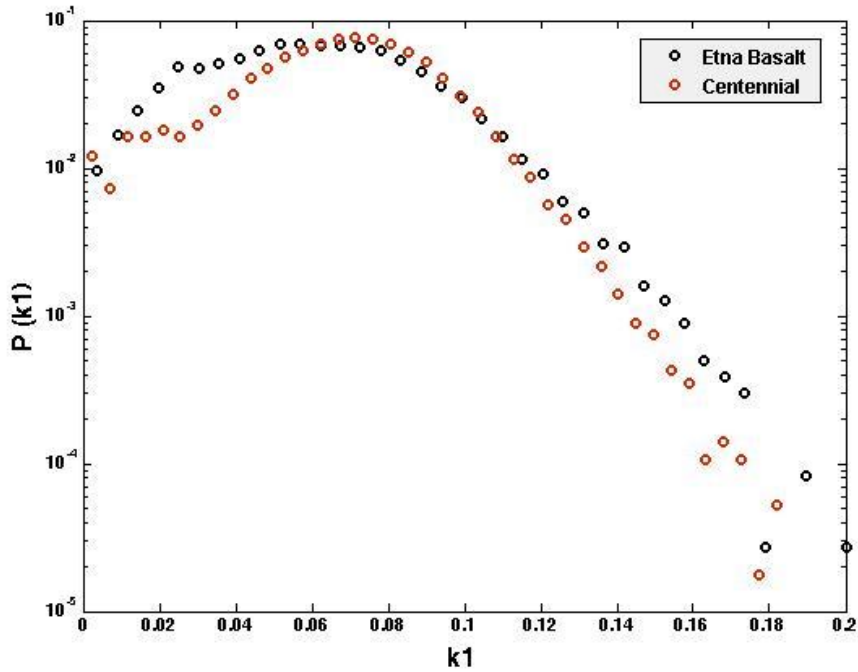
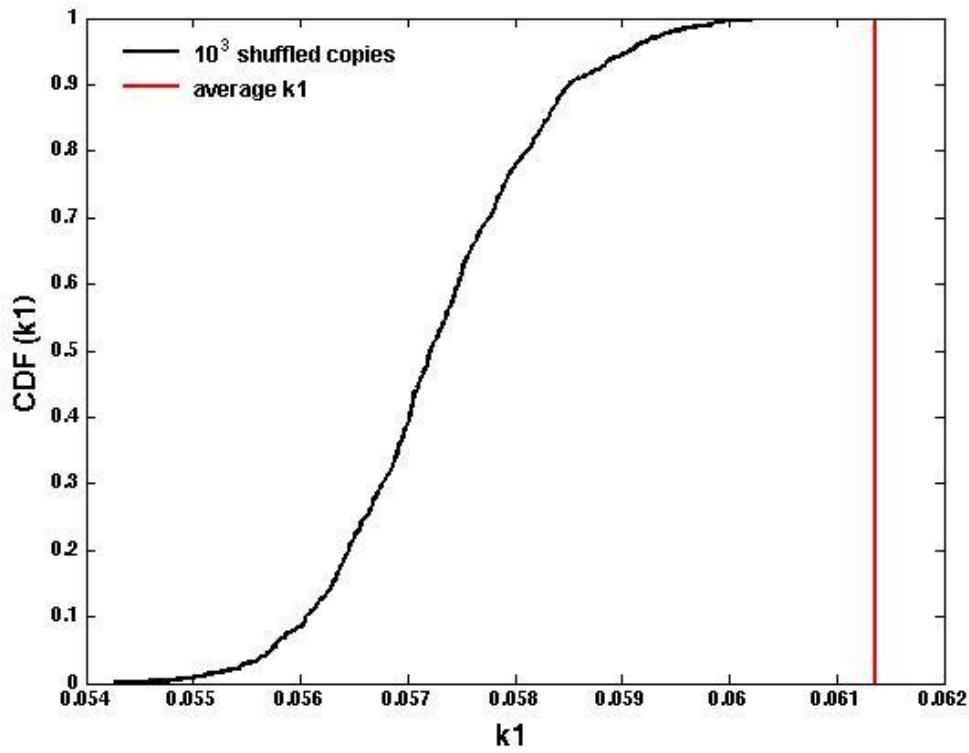


Figure 4.

The cumulative distribution function(CDF) $F(\kappa_1)$ obtained upon randomly shuffling 10^3 times the acoustic emissions catalogue and estimating $E(\kappa_{1,shuffle})$ using $l=6$ to 40 in each case. The (red) vertical line indicates the average value of κ_1 of the original AE catalogue which is far enough from the values obtained from the randomly shuffled copies.



References

- [1] CHAKRABARTI B. K. and BENGUIGUI, L. G., *Statistical Physics of Fracture and Breakdown in Disordered Systems* (Oxford Science Publications, Oxford), 1997
- [2] D. Sornette, *Critical Phenomena in the Natural Sciences: Chaos, Fractals, Self organization, and Disorder: Concepts and Tools* (Springer-Verlag, Berlin, Heidelberg, 2000).
- [3] KRAJCINOVIC D. and VAN MIER J. G. M., *Damage and Fracture of Disordered Materials* (Springer-Verlag, New York), 2000
- [4] MEREDITH P.G., MAIN I. G. and JONES C., *Tectonophysics* **175** (1990) 249.
- [5] TURCOTTE D.L., NEWMAN W. I. and SHCHERBAKOV R., *Geophys. J. Int.* **152**, (2002) 718.
- [6] RUNDLE J.B., *J. Geophys. Res.* **94**, (1989) 2839.
- [7] BENSON P.M., VINCIGUERRA S., MEREDITH P. G., and YOUNG R. P., *Science* **322** (2008) 249.
- [8] BENSON P.M., THOMPSON B. D., MEREDITH P. G., VINCIGUERRA S. and YOUNG R. P., *Geophys. Res. Lett.* **34** (3), (2007) L03303
- [9] BURLINI L., VINCIGUERRA S., DI TORO G., DE NATALE G., MEREDITH P. G., and BURG J.P., *Geology* **35** (2007) 183.
- [10] F. Vallianatos, P. Benson, P. Meredith and P. Sammonds Experimental evidence of a non-extensive statistical physics behaviour of fracture in triaxially deformed Etna basalt using acoustic emissions *EPL*, **97** (2012) 58002 doi: 10.1209/0295-5075/97/58002
- [11] A. Buchel and J. P. Sethna, *Phys. Rev. E.*, **55**, 7669, 1997
- [12] S. Zapperi, P. Ray, H. E. Stanley and A. Vespignani, *Phys. Rev. Lett.*, **78**, 1408, 1997
- [13] F. Kum and H. J. Herrmann, *Phys. Rev. E.*, **59**, 2623, 1999
- [14] S. Gluzman and D. Sornette, *Phys. Rev. E.*, **63**, 066129, 2001
- [15] J. B. Rundle, D. L. Turcotte, R. Shcherbakov, W. Klein and C. Sammis, *Rev. Geophys.* **41**, 1019, 2003
- [16] P. A. Varotsos, N. V. Sarlis, and E. S. Skordas, *Pract. Athens Acad.* **76**, 294 (2001).
- [17] P. A. Varotsos, N. V. Sarlis, and E. S. Skordas, *Phys. Rev. E* **66**, 011902 (2002).
- [18] P. A. Varotsos, N. V. Sarlis, and E. S. Skordas, *Natural Time Analysis: The New View of Time. Precursory Seismic Electric Signals, Earthquakes and other Complex Time-Series* (Springer-Verlag, Berlin, Heidelberg, 2011).
- [19] S. Abe, N. V. Sarlis, E. S. Skordas, H. K. Tanaka, and P. A. Varotsos, *Phys. Rev. Lett.* **94**, 170601 (2005).
- [20] P. A. Varotsos, N. V. Sarlis, E. S. Skordas, H. K. Tanaka, and M. S. Lazaridou, *Phys. Rev. E* **74**, 021123 (2006).
- [21] cristopoulos sarlis
- [22] P. A. Varotsos, N. V. Sarlis, E. S. Skordas, H. K. Tanaka, and M. S. Lazaridou, *Phys. Rev. E* **73**, 031114 (2006)
- [23] N. V. Sarlis, E. S. Skordas, M. S. Lazaridou, and P. A. Varotsos, *Proc. Jpn. Acad., Ser. B* **84**, 331 (2008).
- [24] S. Uyeda, M. Kamogawa, and H. Tanaka, *J. Geophys. Res.* **114**, B02310, doi:10.1029/2007JB005332 (2009).
- [25] N. V. Sarlis, E. S. Skordas, and P. A. Varotsos, *Phys. Rev. E* **80**, 022102 (2009).
- [26] N. V. Sarlis, E. S. Skordas, and P. A. Varotsos, *EPL* **91**, 59001 (2010).
- [27] N. V. Sarlis, E. S. Skordas, and P. A. Varotsos, *Phys. Rev. E* **82**, 021110 (2010).
- [28] P. Varotsos, N. Sarlis, and E. Skordas, *EPL* **96**, 59002 (2011).
- [29] N. V. Sarlis, P. A. Varotsos, and E. S. Skordas, *Phys. Rev. B* **73**, 054504 (2006).
- [30] P. Varotsos, N. V. Sarlis, E. S. Skordas, S. Uyeda, and M. Kamogawa, *Proc. Natl. Acad. Sci. U.S.A.* **108**, 11361 (2011).
- [31] N. Sarlis, E. Skordas, and P. Varotsos, *EPL* **96**, 28006 (2011).
- [32] N. Sarlis, E. Skordas, and P. Varotsos, *Tectonophysics* **513**, 49 (2011).
- [33] Vallianatos, F., Telesca, L., (ed.) 2012. Statistical mechanics in earth physics and natural hazards. *Acta Geophys.* **60**, 499-501.